RSC Advances

This article can be cited before page numbers have been issued, to do this please use: C. Han, Y. Chou, S. Chen and H. Lin, *RSC Adv.*, 2016, DOI: 10.1039/C5RA26827C.

ROYAL SOCIETY OF CHEMISTRY

www.rsc.org/advances

View Article Online
DOI: 10.1039/C5RA26827C

RSC Advances

RSCPublishing

ARTICLE

Hydrogen-bonded bent-core blue phase liquid crystal complexes containing various molar ratios of proton acceptors and donors

Cite this: DOI: 10.1039/x0xx00000x

Received ooth January 2012,
Accepted ooth January 2012

DOI: 10.1039/x0xx00000x

www.rsc.org/

Chun-Chieh Han, Yu-Chaing Chou, San-Yuan Chen and Hong-Cheu Lin*

Various hydrogen-bonded (H-bonded) bent-core liquid crystal complexes consisting of pyridyl and benzoic acid derivatives were synthesized and compared with their covalent analogues in this study. The molar ratios of pyridyl and benzoic acid derivatives could be tuned to form various H-bonded liquid crystal (LC) diads (with 1:1 molar ratio of H-accepters **T** and H-donors **D**) and complexes (with different molar ratios of **T** and **D**). By insertion of H-bonds into different positions of bent-core supramolecules, the mesophasic properties of H-bonded bent-core LC complexes were optimized, which could facilitate the most suitable LC components and compositions to be utilized in H-bonded blue phase (BP) LC complexes. In BPLC complexes, the molar ratios, alkyl chain lengths, the lateral fluoro-substitution and the chiral center of H-bonded bent-core supramolecules would affect their temperature ranges of BPs. Accordingly, H-bonded bent-core complex $\mathbf{P_{III}C_9/A_{II}F^*}$ (3/7 mol/mol) displayed the widest BPI ranges of ΔT_{BPI} = 12.0°C at the correspondent H-accepter **T** = $\mathbf{P_{III}C_9}$ and H-donor **D** = $\mathbf{A_{II}F^*}$. Since the covalent-bonded bent-core mixture only had narrow ranges of BPIII, we could summarize that the introduction of H-bonds in the bent-core center effectively stabilize the BPs and easier induce the BPI.

Introduction

With the chiral nematic (N*) phase induced by the chiral effects of molecular structures, the blue phases (BPs) are the special forms of the chiral nematic phase. The molecular structures of the BPs consist of double twist cylinders (DTCs),[1,2] and the BPs materials often have high chiralities. According to previous researches (e.g., the Kossel diagram method,[3,4] Landau theory[5,6] and the polarized optical microscopy), the BPs can be categorized into three types: BPI, BPII and BPIII with body-centered cubic, simple cubic and amorphous symmetric structures, respectively.[7-10] Since the BPs (e.g., BPI and BPII) possess optically exotic structures, exhibiting no birefringence but selective reflection of circularod-likey polarized light,[11,12] the BPs are utilized on new applications of liquid crystals (LCs), such as fast light modulators, large-screen flat panel displays,[13,14] three-dimensional BP lasers[15-17] and tunable photonic band gap materials.[18-20] However, the main defect of BPs is the narrow stable temperature range, usually less than a few degrees (°C) between the isotropic and chiral nematic phases upon cooling.[21]

Accordingly, several methods were applied to introduce or extend the temperature ranges of BPs by the addition of external materials (e.g., reactive monomers[22-25] and nanoparticles.[26,27]) or the introduction of biaxialities to LC materials (e.g., bent-core LCs,[28-32] hydrogen-bonded LCs[33-35] and LC diads.[36-39]). In addition, some other methods, including the techniques of supercooled freezing,[40] discotic LCs[41] and light induction,[42,43] were also utilized. Therefore, not only developing single components with broad BP ranges are significant,[44-46] but also applying different mixture techniques to extend BP ranges are important. Because of this reason, the interactions of individual components in LC mixtures are of interest to optimize the BP ranges effectively.

Previously, bent-core liquid crystal materials were widely applied in ferroelectric LC materials,[47] organic/inorganic composites[48,49] and chiral nanostructures.[50-52] Recently, the introduction of biaxialities to LC materials, such as: bent-core and di-mesogenic LCs, can induce BPs in LC mixtures. In general, the BPLC mixtures often consist of LC hosts and chiral dopants, where the utilized LC hosts are generally the nematic or chiral nematic phases. Since the nematics of bent-core molecules have special properties compared with the

Department of Materials Science and Engineering, National Chiao Tung University, Hsinchu, Taiwan. Fax: (+886)35724727 E-mail: linhc@mail.nctu.edu.tw

Footnotes relating to the title and/or authors should appear here.
Electronic Supplementary Information (ESI) available: [details of any supplementary information available should be included here]. See DOI: 10.1039/x0xx00000x

View Article Online
DOI: 10.1039/C5RA26827C Journal Name

nematics of rod-like molecules, such as: (a) an increase of twisting power in the N* phase by the introduction of achiral bent-core molecules,[53,54] and (b) many research results suggested the biaxial shape (e.g., bent-core) of the molecules is responsible for the stabilization of DTC structures.[55-57] Therefore, the bent-core molecules are widely used in BPLC mixtures as LC hosts or chiral dopants.

The hydrogen bonds are generated by the attractions of proton donors and acceptors between complimentary polar units intermolecularly or intramolecularly.[58,59] The intermolecular hydrogen bonds of supramolecules can be formed by H-acceptors (e.g., pyridine) and H-donors (e.g., acid).[60-62] However, dimeric supramolecules can be formed by self-intermolecular hydrogen-bonds between two acid moieties of the same molecular structure. Therefore, the H-bonded LC mixtures can be formed via self-assembly of supramolecular force with diversified molecular structures via H-bonds. In addition, the proportions of H-bonded LCs covered various molar ratios (0-100 mol%), and the compatibility between different components also can be solved. In the previous research, the H-bonds can not only generate soft functional segments in LC materials, but also offer stabilized BPLCs.[64-66] Moreover, the location of H-bonds (i.e., the inserted positions of H-bonds in molecules) can monitor the phase transitions and temperature ranges of LCs (including bent-core LCs).[67-69]

In this study, we synthesized two covalent-bonded bent-core molecules and several series of H-bonded bent-core supramolecules containing four pyridyl and benzoic acid derivatives for this study. The molar ratios of pyridyl and benzoic acid derivatives could be tuned to form various LC complexes with over-supplied benzoic acids behaving as rod-like dimers. By insertion H-bonds into different positions of the bent-core supramolecules, the mesophasic properties of H-bonded bent-core molecules were optimized, which could facilitate the most suitable LC components and compositions to be utilized in the H-bonded BPLC complexes. In the BPLC complexes, the molar ratios, alkyl chain lengths, the lateral fluoro-substitution and the chirality of H-bonded bent-core molecules will be discussed for their influences on the temperature ranges of BPs.

Experimental

Chemical analysis

^{1}H NMR spectra were recorded on a Bruker Unity 300 MHz spectrometer using $CDCl_3$ as solvent. Elemental analyses (EA) were performed on a Heraeus CHN-OS RAPID elemental analyzer.

Liquid-crystalline and physical properties

Mesophasic textures of all H-bonded dimeric bent-core complexes and H-bonded mixtures were characterized by polarizing optical microscopy (POM) using a Leica DMLP equipped with a temperature control hot stage (Mettler Toledo FP82HT). Temperatures and enthalpies of phase transitions were determined by differential scanning calorimetry (DSC, model: Perkin Elmer Pyris 7) under N_2 at a heating and cooling rate of 0.5°C min^{-1}. Fourier transform infrared (FTIR) spectra were recorded on a PerkinElmer spectrum 1000. The UV-Vis spectra were recorded on a JASCO V-670 spectrometer with 2 nm resolution at room temperature.

Preparation of materials

The synthesis of covalent-bonded bent-core molecule (**$P_{III}C_9A_{II}F$***), pyridyl derivative (**$P_{III}C_9$**), and benzoic acid derivative (**$A_{II}F$***) were shown in Scheme 1.

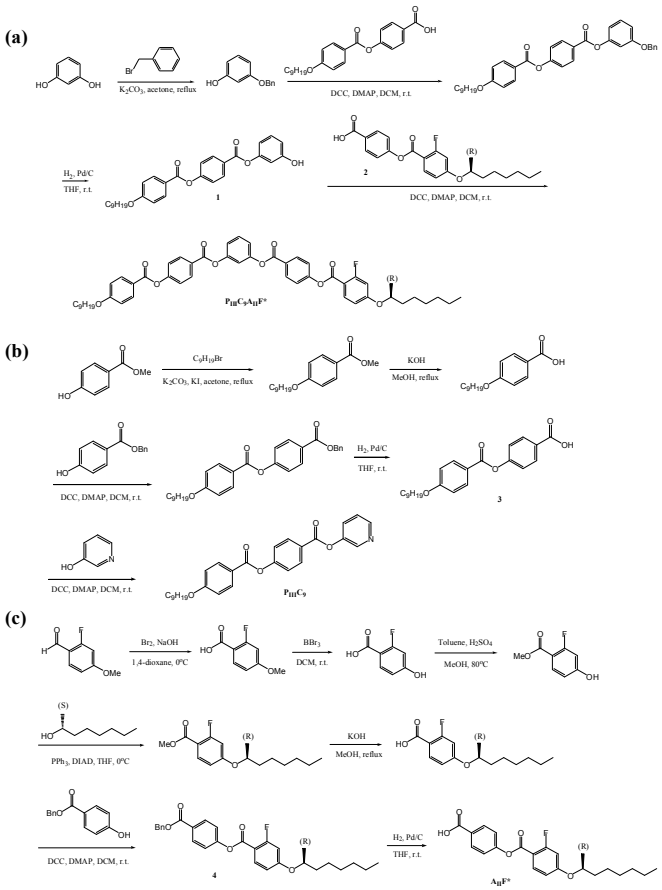

Scheme 1 Synthesis of (a) covalent-bonded bent-core molecule (**$P_{III}C_9A_{II}F$***), (b) H-accepter (**$P_{III}C_9$**) and (c) H-donor (**$A_{II}F$***). (The additional synthetic details are shown in Schemes S1-S3.)

(i) Covalent-bonded bent-core molecule $P_{III}C_9A_{II}F$*. A mixture of compound **1** (5.67g, 11.9mmole), compound **2** (4.62g, 11.9mmole), DMAP (0.18 g, 1.5 mmole) and DCC (4.11 g, 19.8mmol) was dissolved in dry DCM under nitrogen for 16 h at room temperature. After work up, the solvent was extracted with water/DCM and organic liquid layer was dried over anhydrous magnesium sulphate. After removal of the solvent by evaporation under reduced pressure, the residue was purified by column chromatography and recrystallized from DCM/*n*-hexane to afford compound **$P_{III}C_9A_{II}F$*** was obtained as a white solid in 80% yield. ^{1}H NMR (300 MHz, $CDCl_3$): δ (ppm) 8.25 (d, J = 8.4 Hz, 4H, Ar-H),8.13 (d, J = 8.7 Hz, 2H,

Journal Name
View Article Online
DOI: 10.1039/C5RA26827C
ARTICLE

Ar-H), 7.99 (t, *J* = 8.7 Hz, 1H, Ar-H),7.46 (t, *J* = 8.4 Hz, 1H, Ar-H), 7.36 (d, *J* = 8.4 Hz, 4H, Ar-H), 7.18 (m, 3H,Ar-H), 7.13 (d, *J* = 8.7 Hz, 2H, Ar-H), 6.75-6.64 (m, 2H, Ar-H), 4.43(m, 1H, -OCH-), 4.03 (t, *J* = 6.5 Hz, 2H, -OCH_2-), 1.49-1.23 (m, 26H, -CH_2-), 0.87 (m, 6H, -CH_3). Anal. calcd for $C_{51}H_{55}FO_{10}$: C, 72.32, H, 6.55; found: C, 73.19, H, 6.97%.

(ii) H-accepter $P_{III}C_9$. A mixture of compound **3** (4.58g, 11.9mmole), 3-hydroxypyridine (1.13 g, 11.9 mmole), DMAP (0.18 g, 1.5 mmole) and DCC (4.11 g, 19.8mmol) was dissolved in dry DCM under nitrogen for 16 h at room temperature. After work up, the solvent was extracted with water/DCM and organic liquid layer was dried over anhydrous magnesium sulphate. After removal of the solvent by evaporation under reduced pressure, the residue was purified by column chromatography and recrystallized from DCM/*n*-hexane to afford compound **$P_{III}C_9$** was obtained as a white solid in 69% yield. ^{1}H NMR (300 MHz, $CDCl_3$): δ (ppm) 8.56 (m, 2H, Ar-H), 8.29 (d, *J* = 9.0 Hz, 2H, Ar-H), 8.15 (d, *J* = 9.0 Hz, 2H, Ar-H), 7.64 (m, 1H, Ar-H), 7.40-7.25 (m, 3H, Ar-H), 6.98 (d, *J* = 9.0 Hz, 2H, Ar-H), 4.05 (t, *J* = 6.5 Hz, 2H, -OCH_2-), 1.85-1.78 (m, 2H, -CH_2-), 1.548-1.22 (m,12H, -CH_2-), 0.90 (t, *J* = 6.3 Hz, 3H, -CH_3). Anal. calcd for $C_{28}H_{31}NO_5$: C, 72.86, H, 6.77, N, 3.03; found: C, 72.85, H, 6.86, N, 3.22%.

(iii) H-donor $A_{II}F^*$. Into a 500 ml round bottom two-neck flask compound **4** (10 g, 20 mmole) and 15% Pd/C (1.5 g) catalyst were stirred in THF (200 ml) under hydrogen at room temperature for overnight. The catalyst was removed by filtration through Celite and washed with THF. The solvent was removed by evaporation under reduced pressure and the crude product recrystallized by THF/*n*-hexane to give white solid of **$A_{II}F^*$**, yield 92%. ^{1}H NMR (300 MHz, $CDCl_3$): δ (ppm) 8.16 (d, *J* = 8.7 Hz, 2H, Ar-H), 8.03 (t, *J* = 8.0 Hz, 1H, Ar-H), 7.32 (m, 2H, Ar-H), 6.74 (dd, *J* = 9.0 Hz, 1H, Ar-H), 6.68 (dd, *J* = 11.7 Hz, 1H, Ar-H), 4.42 (m, 1H, -OCH-), 1.71-1.60 (m, 2H, -CH_2-), 1.33-1.27 (m, 11H, -CH_2CH_3), 0.86 (t, *J* = 6.3 Hz, 3H, -CH_3). Anal. calcd for $C_{22}H_{25}FO_5$: C, 68. 03, H, 6.49; found: C, 67.78, H, 6.44%. The remaining compounds and experimental procedures were shown in supporting information.

Preparation of samples

All H-bonded dimeric bent-core complexes and H-bonded mixtures were constructed by mixing appropriate molar ratios of H-acceptors and H-donors in solutions of dry THF, which were self-assembled into H-bonded supramolecules or mixtures by evaporating solvents slowly.

Results and discussion

Several series of H-bonded bent-core supramolecular complexes (**T/D**) were synthesized and prepared by mixing different molar ratios of proton acceptors **T** (pyridyl derivatives) and proton donors **D** (benzoic acid derivatives). As shown in Fig. 1a, these supramolecular complexes (**T/D**) consist of four proton acceptors **T** (**$P_{IV}C_9$**, **$P_{III}C_5$**, **$P_{III}C_7$** and **$P_{III}C_9$**) and four proton donors **D** (**A_IF^***, **$A_{II}F$**, **A_{II}^*** and **$A_{II}F^*$**), where **A**, *, **F**, **P** and subscripts of Arabic (5, 7 and 9) and Roman (**I**, **II** and **III**) numerals denote the acid, chiral, fluoro, pyridyl moieties, carbon numbers and phenyl ring numbers, respectively. In addition, two covalent-bonded bent-core analogues **$P_{III}C_5A_{II}F^*$** and **$P_{III}C_9A_{II}F^*$** (see Fig. 1b) were also synthesized to be prepared in this study. As the molar ratio of proton acceptor and donor is equal to 1:1, these H-bonded bent-core supramolecular complexes were self-assembled to form supramolecular diads, i.e., **T/D** = 1/1 mol. In the meanwhile, the proton donors **D** will be self-assembled to generate H-bonded rod-like dimmers (see Fig. 1c).

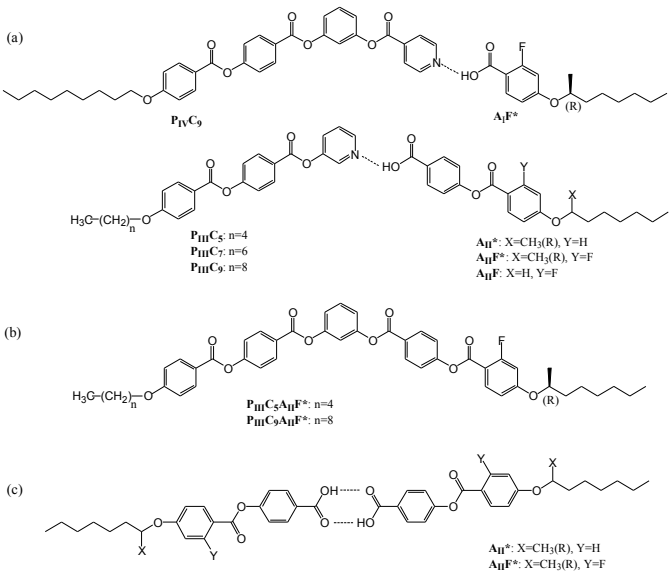

Fig. 1 Molecular structures of (a) H-bonded bent-core supramolecular complexes **T/D** with various ratios of H-acceptors **T** and H-donors **D**, where **T** = **$P_{IV}C_9$**, **$P_{III}C_5$**, **$P_{III}C_7$** and **$P_{III}C_9$**; **D** = **A_IF^***, **$A_{II}F$**, **A_{II}^*** and **$A_{II}F^*$**, (b) covalent-bonded bent-core analogues **$P_{III}C_5A_{II}F^*$** and **$P_{III}C_9A_{II}F^*$**, (c) H-bonded rod-like dimers **D**.

Mesophasic properties

The phase transition temperatures, enthalpies and mesophasic ranges of all H-bonded bent-core diads **T/D** (1/1) are demonstrated in Tables 1 and S1, which were characterized by differential scanning calorimetry (DSC) and polarizing optical microscopy (POM). The transition temperatures of blue phase I (BPI) – chiral nematic phases (N*) was determined by POM (at a cooling rate of 0.5°C min^{-1}) due to their undetectable enthalpy changes by DSC upon cooling. The H-bonded bent-core diads **T/D** (1/1) were self-assembled by two complimentary components of H-acceptors (**T**) and H-donors (**D**) with a stronger interactrion of –OH···N to replace –OH···C=O– of self-dimeric H-donors. Since the over-supplied proton acceptors **T** will eliminate the liquid crystallinity of supramolecular complexes (**T/D**), only the improved mesophasic properties of over-supplied proton donors **D** in supramolecular complexes are of our concern, which is because the over-supplied proton donors **D** will be self-assembled to generate H-bonded rod-like dimmers coexisting with their miscible supramolecular diads. The configurational influences of various H-bonded bent-core diads (**T/D** = 1/1) and H-bonded complexes (**T/D** ≠ 1/1),

View Article Online
DOI: 10.1039/C5RA26827C
Journal Name

Table 1 Phase transition temperatures (°C) and enthalpies (J g^{-1})[a,b] of H-bonded bent-core diads and covalent-bonded bent-core analogue upon cooling.

Complex (mol/mol)	Phase transition temperature upon cooling (°C) [enthalpies (KJ mol^{-1})]
$P_{IV}C_9/A_IF^*$ = 1:1	Iso 110.6°C [1.98] K
$P_{III}C_9/A_{II}F^*$ = 1:1	Iso 92.7°C [1.34] N* 62.3°C [1.64] K
$P_{III}C_9/A_{II}^*$ = 1:1	Iso 101.3°C [1.03] N* 87.6°C [1.48] K
$P_{III}C_9A_{II}F^*$	Iso 127.3°C [3.51] K

[a]Peak temperatures in DSC profiles obtained during the first cooling at a rate of 1°C min^{-1}. [b]Iso = isotropic phase; N* = chiral nematic phase; K = crystalline phase.

including numbers of aromatic rings, positions of H-bonds, alkyl chain lengths of H-acceptors **T**, and chiral center along with lateral fluoro substituent of H-donors **D**, on mesophasic properties are discussed as follows:

(i) H-bonded bent-core diads $P_{IV}C_9/A_IF^*$, $P_{III}C_9/A_{II}F^*$, $P_{III}C_9/A_{II}^*$ (where T/D = 1:1) and the covalent-bonded bent-core analogue $P_{III}C_9A_{II}F^*$. As shown in Table 1, H-bonded bent-core diads $P_{IV}C_9/A_IF^*$ and $P_{III}C_9/A_{II}F^*$ had similar chemical structures as their covalent-bonded bent-core analogue $P_{III}C_9A_{II}F^*$, but the positions of H-bonds in H-bonded bent-core diads $P_{III}C_9/A_{II}F^*$ and $P_{IV}C_9/A_IF^*$ are different, where the H-bond of $P_{III}C_9/A_{II}F^*$ was near the center of the bent-core structure. The H-bonded bent-core diad $P_{IV}C_9/A_IF^*$ didn't possess LC phases upon both heating and cooling, and its isotropization point (110.6°C) was higher than that (92.7°C) of $P_{III}C_9/A_{II}F^*$. However, the H-bonded bent-core diad $P_{III}C_9/A_{II}F^*$ had a very wide chiral nematic phase with a phase range wider than 30°C upon cooling. Hence, the H-bond near the center of the bent-core structure in H-bonded bent-core diad $P_{III}C_9/A_{II}F^*$ generated a softer H-bonded linkage than that far away from the center (with a more rigid bent core) in H-bonded bent-core diad $P_{IV}C_9/A_IF^*$, and the reduced ordered bent-core stacking of H-boned diad $P_{III}C_9/A_{II}F^*$ would facilitate the mesophasic formation more easily. The effects of the lateral fluoro-substitution on H-boned diad $P_{III}C_9/A_{II}F^*$ was compared with the analogous H-bonded diad $P_{III}C_9/A_{II}^*$ (without fluoro-substitution). As expected, the H-bonded diad $P_{III}C_9/A_{II}F^*$ with the lateral fluoro-substitution had a wider chiral nematic phase range (ΔT_{N^*} = 30.4°C) and lower phase transition temperatures than $P_{III}C_9/A_{II}^*$ (ΔT_{N^*} = 13.7°C). Compared with H-bonded bent-core diads $P_{IV}C_9/A_IF^*$ and $P_{III}C_9/A_{II}F^*$, the covalent-bonded bent-core analogue $P_{III}C_9A_{II}F^*$ didn't show any LC phases upon both heating and cooling, and $P_{III}C_9A_{II}F^*$ had the highest isotropization temperature at 127.3°C due to the highest rigidity of its covalent structure. Not only the positions of H-bonds but also the lateral fluoro-substitution affected the chiral nematic phase range in H-bonded bent-core diads **T/D** (1:1). Therefore, the H-bonded bent-core diad $P_{III}C_9/A_{II}F^*$ illustrated the widest chiral nematic phase range and lowest phase transition temperatures among these molecules with analogous H-bonded and covelent-bonded bent-core structures.

(ii) H-bonded bent-core complexes $P_{III}C_5/A_{II}F^*$, $P_{III}C_7/A_{II}F^*$ and $P_{III}C_9/A_{II}F^*$ (where T = $P_{III}C_5$, $P_{III}C_7$ and $P_{III}C_9$ with different alkyl chain lengths; D = $A_{II}F^*$).

Since the H-bonded bent-core diad $P_{III}C_9/A_{II}F^*$ revealed the widest chiral nematic phase range, we tried to improve the mesophasic properties by the over-supply of proton donor **D** = $A_{II}F^*$ in the analogous supramolecular complexes (**T** = $P_{III}C_5/A_{II}F^*$, $P_{III}C_7/A_{II}F^*$ and $P_{III}C_9/A_{II}F^*$) with different alkyl chain lengths, where the over-supplied proton donor $A_{II}F^*$ will be self-assembled to generate H-bonded rod-like dimmers coexisting with their miscible supramolecular diads. As shown in Figs. 2(a)-2(c), the H-bonded bent-core complexes **T/D** (where **T** = $P_{III}C_5$, $P_{III}C_7$ and $P_{III}C_9$; **D** = $A_{II}F^*$) were prepared with various molar ratios of excessive H-donor $A_{II}F^*$. We can summarize the following effects on the mesophasic ranges of blue phases for all H-bonded bent-core complexes $P_{III}C_5/A_{II}F^*$, $P_{III}C_7/A_{II}F^*$ and $P_{III}C_9/A_{II}F^*$ containing different alkyl chain lengths of H-accepters **T** and the same H-donor **D** = $A_{II}F^*$, i.e., molar ratio effects of H-donor and H-acceptors; symmetry effects of alkyl chain lengths on H-donor and H-acceptors; alkyl chain length effects of H-acceptors; effects of covalent- and H-bonded bent-core mixtures.

(a) Molar ratio effects of H-donor and H-acceptors. Since all H-bonded bent-core diads $P_{III}C_5/A_{II}F^*$, $P_{III}C_7/A_{II}F^*$ and $P_{III}C_9/A_{II}F^*$ (where **T/D** = 1:1) do not possess any BP phases, the H-bonded bent-core complexes **T/D** were compared with various molar ratios of excessive H-donor $A_{II}F^*$. As shown in Figs. 2(a)-2(c), the BPI was induced in all H-bonded bent-core complexes $P_{III}C_5/A_{II}F^*$, $P_{III}C_7/A_{II}F^*$ and $P_{III}C_9/A_{II}F^*$ at the molar ratios of H-donor $A_{II}F^*$ ranging 55-75 mol%, 55-70 mol% and 55-80 mol%, respectively. The BPI ranges showed a tendency of increasing first then decreasing later from 55 mol% to 70-80 mol% of H-donor $A_{II}F^*$, and $P_{III}C_9/A_{II}F^*$ had the widest molar ratios (55-80 mol%) of H-donor $A_{II}F^*$ to present the BPI. Among these H-bonded bent-core complexes with excessive H-donor $A_{II}F^*$, $P_{III}C_9/A_{II}F^*$ possessed the widest BPI range of ΔT_{BPI} = 12.0°C at $A_{II}F^*$ = 70 mol%. In addition, more information of H-bonded bent-core complexes $P_{IV}C_9/A_IF^*$ with various molar ratios of H-donor A_IF^* is shown in Fig. S1, where no BP phase is observed if the H-bonded position is away from the bent-core center. Hence, the slightly excessive H-donor $A_{II}F^*$ would increase the chiral concentration to induce BPI in all H-bonded bent-core complexes $P_{III}C_5/A_{II}F^*$, $P_{III}C_7/A_{II}F^*$ and $P_{III}C_9/A_{II}F^*$, but high molar ratios H-donor $A_{II}F^*$ over 80 mol% would cause the disappearance of the BPI due to the biaxial dilution of the over-supplied uniaxial rod-like dimer $A_{II}F^*$.

(b) Alkyl chain length effects of H-acceptors. Among all H-bonded bent-core complexes in Figs. 2(a)-2(c), $P_{III}C_7/A_{II}F^*$ possesses the BPI phase with the narrowest molar ratio ranges of H-donor $A_{II}F^*$ (i.e., 55-70 mol%) due to the symmetrical alkyl chain length on both H-donor $A_{II}F^*$ and H-acceptor $P_{III}C_7$. Comparing H-bonded bent-core complexes $P_{III}C_5/A_{II}F^*$ and $P_{III}C_9/A_{II}F^*$ with asymmetrical alkyl chain lengths, the molar ratio ranges of H-donor with BPI (55-75 mol% and 55-80 mol%, respectively) were also extended by increasing the alkyl chain length of H-acceptor. Furthermore, H-bonded bent-core complexes $P_{III}C_5/A_{II}F^*$, $P_{III}C_7/A_{II}F^*$ and $P_{III}C_9/A_{II}F^*$ displayed the widest BPI ranges of ΔT_{BPI} = 10.8°C, 11.6°C and 12.0°C, at the correspondent molar ratios of H-donor $A_{II}F^*$ = 70 mol%, 60 mol% and 70 mol%, respectively. Therefore, the

Journal Name

View Article Online
DOI: 10.1039/C5RA26827C

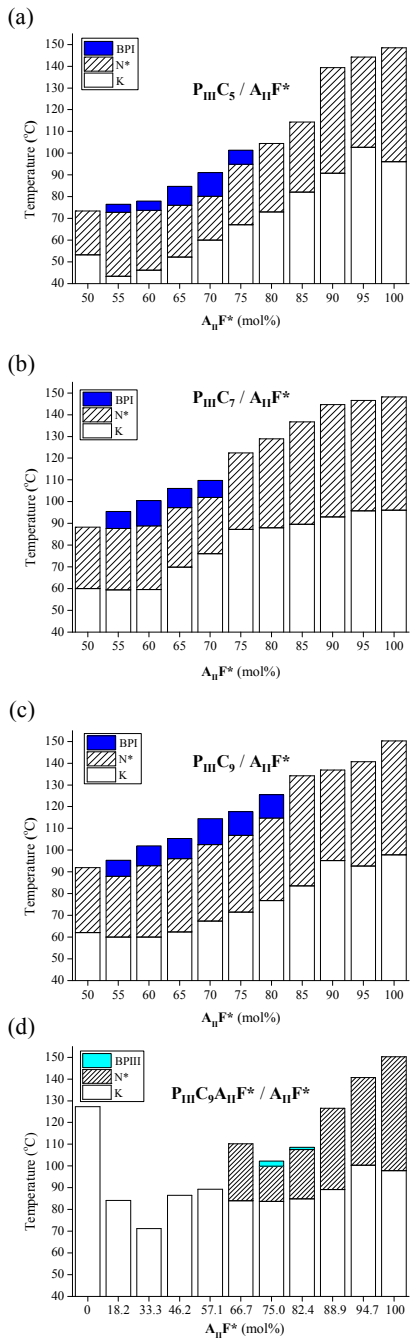

Fig. 2 Binary phase diagrams of H-bonded bent-core complexes (a) $\mathbf{P_{III}C_5/A_{II}F^*}$, (b) $\mathbf{P_{III}C_7/A_{II}F^*}$, (c) $\mathbf{P_{III}C_9/A_{II}F^*}$ and covalent-bonded bent-core mixture $\mathbf{P_{III}C_9A_{II}F^*/A_{II}F^*}$ with different molar ratios of $\mathbf{A_{II}F^*}$. The POM observations and DSC measurements were carried out at a cooling rate of 0.5°C min^{-1} (Table S1 and S2). I: isotropic phase; BPI: blue phase I; N*: chiral nematic phase; K: crystalline phase.

BPI ranges (ΔT_{BPI}) of H-bonded bent-core complexes were affected by the alkyl chain length of H-accepter, where the longer alkyl chain length the wider BPI ranges (ΔT_{BPI}), i.e., $\mathbf{P_{III}C_5/A_{II}F^*} < \mathbf{P_{III}C_7/A_{II}F^*} < \mathbf{P_{III}C_9/A_{II}F^*}$. The symmetrical alkyl chain lengths on both H-donor and H-acceptors played an important role on the molar ratio ranges of H-donor with BPI, but the BPI ranges in H-bonded bent-core complexes were affected by the alkyl chain lengths of H-accepters.

(c) Effects of covalent-bonded bent-core mixture and H-bonded bent-core complex. Regardless of the similar structure as the H-bonded bent-core diad $\mathbf{P_{III}C_9/A_{II}F^*}$ (1/1 mol/mol), the covalent-bonded bent-core analogue $\mathbf{P_{III}C_9A_{II}F^*}$ does not possess any mesophase. Since both of the H-bonded bent-core diad $\mathbf{P_{III}C_9/A_{II}F^*}$ = 1:1 (mol/mol) and its covalent-bonded bent-core analogue $\mathbf{P_{III}C_9A_{II}F^*}$ do not possess any BPs, the H-bonded bent-core complex $\mathbf{P_{III}C_9/A_{II}F^*}$ with proper molar ratios of over-supplied H-donor $\mathbf{A_{II}F^*}$ (55-80 mol%) having the BPI should be compared with its analogous covalent-bonded bent-core mixture $\mathbf{P_{III}C_9A_{II}F^*/A_{II}F^*}$ (with >50 mol% of H-donor $\mathbf{A_{II}F^*}$). As shown in Fig. 2d, the covalent-bonded bent-core analogue $\mathbf{P_{III}C_9A_{II}F^*}$ was used to replace the H-bonded bent-core diad $\mathbf{P_{III}C_9/A_{II}F^*}$ = 1:1, so the molar ratios of H-donor $\mathbf{A_{II}F^*}$ in $\mathbf{P_{III}C_9A_{II}F^*/A_{II}F^*}$ = 0, 18.2, 33.3, 46.2, 57.1, 66.7, 75.0, 82.4, 88.9, 94.7 and 100 mol% are equivalent to the molar ratios of H-donor $\mathbf{A_{II}F^*}$ in $\mathbf{P_{III}C_9/A_{II}F^*}$ = 55, 60, 65, 70, 75, 80, 85, 90, 95 and 100 mol%, respectively. Compared with $\mathbf{P_{III}C_9/A_{II}F^*}$ possessing the BPI phase at the molar ratios of $\mathbf{A_{II}F^*}$=55-80 mol% shown in Fig. 2a, the covalent-bonded bent-core mixture $\mathbf{P_{III}C_9A_{II}F^*/A_{II}F^*}$ only induced the BPIII phase at molar ratios of $\mathbf{A_{II}F^*}$ = 75.0 to 82.4 mol% in Fig. 2d. Thus, the covalent-bonded bent-core analogue $\mathbf{P_{III}C_9A_{II}F^*}$ (without any mesophase) might play an important role of a biaxial component in the covalent-bonded bent-core mixture $\mathbf{P_{III}C_9A_{II}F^*/A_{II}F^*}$ to induce the BPIII phase. Due to the existence of the chiral nematic phase for the LC host of the H-bonded bent-core diad ($\mathbf{P_{III}C_9/A_{II}F^*}$ = 1:1), the H-bonded bent-core complex $\mathbf{P_{III}C_9/A_{II}F^*}$ possessed the widest blue phase (i.e., ΔT_{BPI} = 12.0°C) at the molar ratio of $\mathbf{A_{II}F^*}$ = 70 mol%. Therefore, both H-bonded bent-core diad $\mathbf{P_{III}C_9/A_{II}F^*}$ = 1:1 and its covalent-bonded bent-core analogue $\mathbf{P_{III}C_9A_{II}F^*}$ have different effects on their LC mixtures containing proper molar ratios of over-supplied H-donor $\mathbf{A_{II}F^*}$ to favor various blue phases, i.e., BPI and BPIII, respectively. Moreover, the bent-core molecules with wider chiral nematic phase (by introducing H-bonds) were also easier to stabilize and induce the BPI in the H-bonded bent-core complexes.

(iii) Effects of fluoro group and chiral center of H-donors on H-bonded bent-core complexes. As shown in Fig. 3, two more hybrid H-bonded complexes $\mathbf{P_{III}C_9/(A_{II}F^*+A_{II}F)}$ and $\mathbf{P_{III}C_9/(A_{II}F^*+A_{II}^*)}$ with dual H-donors (where $\mathbf{T} = \mathbf{P_{III}C_9}$; $\mathbf{D} = \mathbf{A_{II}F^*}$, $\mathbf{A_{II}F}$ and $\mathbf{A_{II}^*}$ are chiral/fluoro, achiral/fluoro and chiral/non-fluoro H-donors, respectively) were prepared to compare the effects of the chiral center and fluoro group of H-donors on H-bonded bent-core complexes in contrast to H-bonded bent-core complex $\mathbf{P_{III}C_9/A_{II}F^*}$ at $\mathbf{A_{II}F^*}$ = 70 mol% (with the widest BPI range of ΔT_{BPI} = 12.0°C). Hence, the total molar ratio of dual H-donors ($\mathbf{A_{II}F^*+A_{II}F}$) and ($\mathbf{A_{II}F^*+A_{II}^*}$) in hybrid H-bonded complexes $\mathbf{P_{III}C_9/(A_{II}F^*+A_{II}F)}$ and $\mathbf{P_{III}C_9/(A_{II}F^*+A_{II}^*)}$ was fixed at 70 mol% (similar to the controlling sample with the widest BPI range). Regarding the contribution of the chiral center of H-donor in hybrid H-bonded complex $\mathbf{P_{III}C_9/(A_{II}F^*+A_{II}F)}$ in Fig. 3a, the BPI ranges were gradually reduced by increasing the molar ratio of $\mathbf{A_{II}F}$ in the dual H-donors ($\mathbf{A_{II}F^*+A_{II}F}$). Finally, the concentration of $\mathbf{A_{II}F^*}$ (replaced with $\mathbf{A_{II}F}$ without the chiral center) was too

View Article Online
DOI: 10.1039/C5RA26827C Journal Name

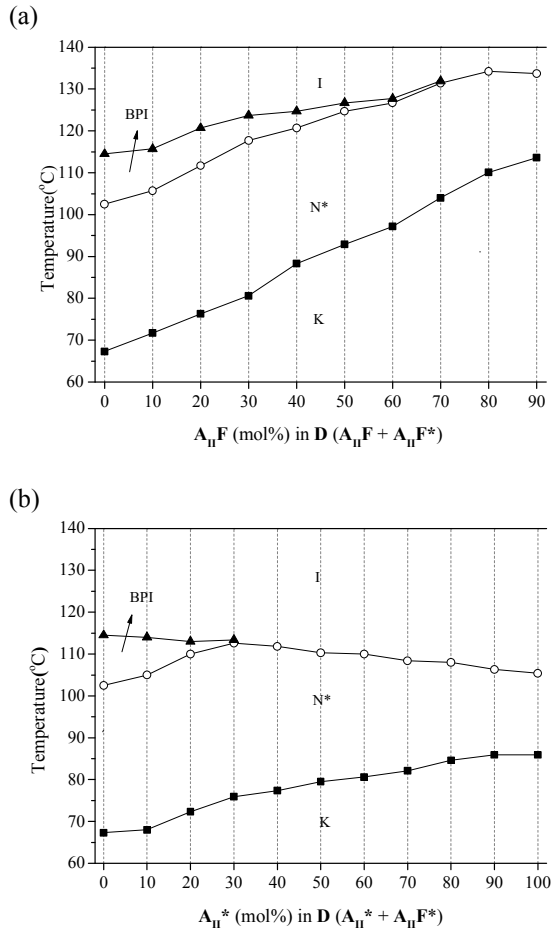

Fig. 3 Binary phase diagrams of hybrid H-bonded complexes $\mathbf{P_{III}C_9/D}$ = 30/70 mol/mol with different molar ratios of $\mathbf{A_{II}F^*}$, where (a) **D** = $\mathbf{A_{II}F}$+$\mathbf{A_{II}F^*}$, (b) **D** = $\mathbf{A_{II}^*}$+$\mathbf{A_{II}F^*}$. The POM observations and DSC measurements were carried out at a cooling rate of 0.5°C min^{-1} (Table S3). I: isotropic phase; BPI: blue phase I; N*: chiral nematic phase; K: crystalline phase.

low to maintain the required chiral concentration in hybrid H-bonded complexes $\mathbf{P_{III}C_9/(A_{II}F^*+A_{II}F)}$ at $\mathbf{A_{II}F^*}$ = 20 mol% (i.e., $\mathbf{A_{II}F}$ = 80 mol%) of the dual H-donor ($\mathbf{A_{II}F^*+A_{II}F}$), so it was not sufficient to sustain the BPI. On the contrary, the contribution of the fluoro group of H-donor in hybrid H-bonded complex $\mathbf{P_{III}C_9/(A_{II}F^*+A_{II}^*)}$ of Fig. 3b was verified that the BPI ranges were more dramatically reduced by increasing the molar ratio of $\mathbf{A_{II}^*}$ in the dual H-donors ($\mathbf{A_{II}F^*+A_{II}^*}$). At last, the concentration of $\mathbf{A_{II}F^*}$ (replaced with $\mathbf{A_{II}^*}$ without the fluoro group) was too low to maintain the polarity in hybrid H-bonded complexes $\mathbf{P_{III}C_9/(A_{II}F^*+A_{II}^*)}$ at $\mathbf{A_{II}F^*}$ = 60 mol% (i.e., $\mathbf{A_{II}^*}$ = 40 mol%) of the dual H-donor ($\mathbf{A_{II}F^*+A_{II}^*}$). The additional information of the total replacement of $\mathbf{A_{II}F^*}$ with $\mathbf{A_{II}^*}$ in the hybrid H-bonded complex $\mathbf{P_{III}C_9/(A_{II}F^*+A_{II}^*)}$ to become $\mathbf{P_{III}C_9/A_{II}^*}$ is shown in Fig. S2. According to Figs. 3a and 3b, the disappearance of BPI in both hybrid H-bonded complexes $\mathbf{P_{III}C_9/(A_{II}F^*+A_{II}F)}$ and $\mathbf{P_{III}C_9/(A_{II}F^*+A_{II}^*)}$ occurred at a higher molar replacement of $\mathbf{A_{II}F^*}$ with $\mathbf{A_{II}F}$ (80 mol% without the chiral center) than that with $\mathbf{A_{II}^*}$ (40 mol% without the fluoro group), so the replacement of the polar fluoro group in the dual H-donor to eliminate BPI is

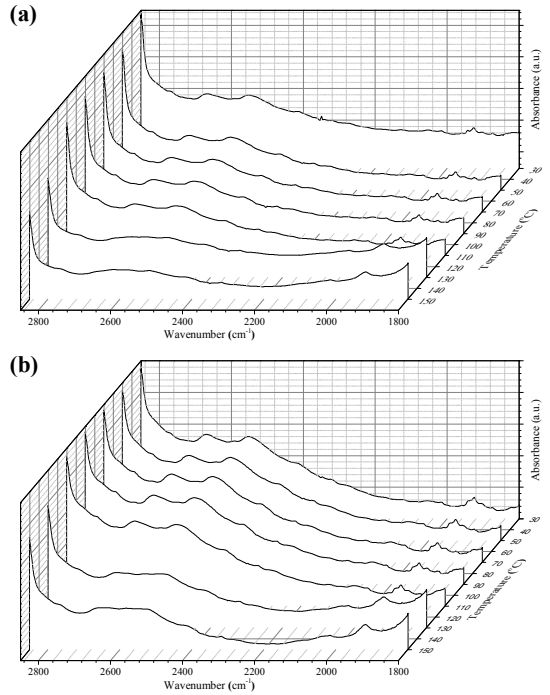

Fig. 4 Temperature dependent FTIR spectra of H-bonded (a) diad $\mathbf{P_{III}C_9/A_{II}F^*}$ = 1/1 mol/mol and (b) complex $\mathbf{P_{III}C_9/A_{II}F^*}$ = 3/7 mol/mol.

more effective than that of the chiral center. Hence, the polar fluoro group of $\mathbf{A_{II}F^*}$ is more important than its chiral center to stabilize the BPI phase in $\mathbf{P_{III}C_9/A_{II}F^*}$.

Characterization of H-bonded structures

As shown in Figs. 4(a) and 4(b), the characteristic peaks of H-bonds formed by carboxylic acid/pyridyl groups could be observed with different extents at various temperatures in the H-bonded bent-core diad $\mathbf{P_{III}C_9/A_{II}F^*}$ (1/1 mol/mol) and complex $\mathbf{P_{III}C_9/A_{II}F^*}$ (3/7 mol/mol), respectively, where the stability of H-bonds in the bent-core diad and complex can be directly confirmed by the temperature-dependent FTIR spectra. During the formation of H-bonds in complexation of $\mathbf{A_{II}F^*}$ (H-donor) with $\mathbf{P_{III}C_9}$ (H-acceptor), the O-H bands of pure $\mathbf{A_{II}F^*}$ (H-donor) centred at about 2560 and 2673 cm^{-1} were shifted to 1927 cm^{-1} and 2550 cm^{-1}, respectively, indicating strong H-bonding formed between the pyridyl and carboxylic acid groups in the asymmetric heterodimers.[70,71] Two H-bonded characteristic peaks centred at about 2550.2 and 1927.3 cm^{-1} showed minor changes at higher temperatures of 130°C and 150°C in Figs. 4(a) and 4(b), which suggests the gradual disappearance of stable H-bonds in diad and complex. On the other hand, the stretching vibration of carboxylic acid group C=O appeared at 1700 cm^{-1} and the stretching vibration of ester carbonyl group C=O appeared at 1726 cm^{-1}. In the H-bonded asymmetric diad of $\mathbf{P_{III}C_9/A_{II}F^*}$ (1/1 mol/mol), a shoulder can be observed in the main peak located at 1726 cm^{-1}. This shoulder is the carbonyl group which is in a less associated state than the pure $\mathbf{A_{II}F^*}$ (H-donor) with a weaker stretching vibration in carboxylic acid group C=O appeared at 1700 cm^{-1}.[72,73] This is attributed to a stretching vibration in carboxylic acid group C=O at 1700 cm^{-1} in the pure H-donor $\mathbf{A_{II}F^*}$ which

View Article Online
DOI: 10.1039/C5RA26827C
ARTICLE

shifts toward a higher wavenumber and overlaps with the band of the ester carbonyl group at 1726 cm^{-1} in the H-bonded asymmetric diad of **$P_{III}C_9/A_{II}F^*$** (1/1 mol/mol). These consequences show that hydrogen bonds were formed between **$A_{II}F^*$** (H-donor) and **$P_{III}C_9$** (H-acceptor) as well as the other H-bonded complexes.

Optical and UV-Vis investigations

The mesophases of H-bonded bent-core diads and complexes were characterized by the photo-images of POM textures at different temperatures, which are illustrated in Figs. 5(a)-5(c) for **$P_{III}C_5/A_{II}F^*$** at 50/50, 35/65 and 30/70 mol/mol, respectively, Figs. 5(d)-5(f) for **$P_{III}C_7/A_{II}F^*$** at 50/50, 40/60 and 35/65 mol/mol, respectively and Figs. 5(g)-5(i) for **$P_{III}C_9/A_{II}F^*$** at 50/50, 35/65 and 30/70 mol/mol, respectively. The chiral nematic phase (N*) and blue phase I (PBI) were confirmed by POM textures with fine stripes and colourful platelets, respectively.

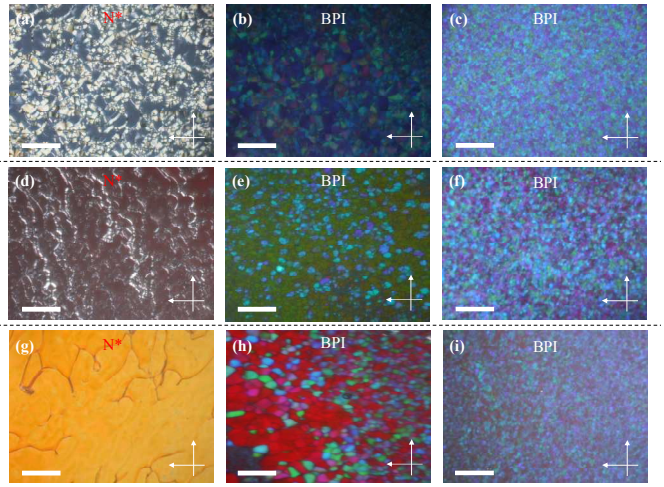

Fig. 5 POM textures of H-bonded bent-core diads and complexes for **$P_{III}C_5/A_{II}F^*$** with (a) 50/50 mol at 60°C, (b) 35/65 mol at 80°C, (c) 30/70 mol at 85°C; **$P_{III}C_7/A_{II}F^*$** with (d) 50/50 mol at 75°C, (e) 40/60 mol at 94°C, (f) 35/65 mol at 102°C; **$P_{III}C_9/A_{II}F^*$** with (g) 50/50 mol at 75°C, (h) 35/65 mol at 100°C, (i) 30/70 mol at 108°C. (Scale bar: 40 μm. White arrows are the directions of polarizers and analyzers)

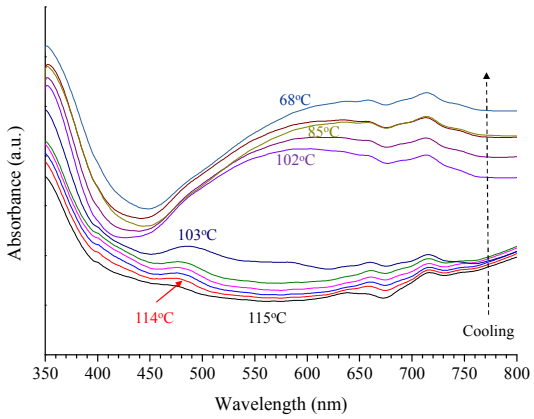

Fig. 6 Absorbance spectral change versus temperature for H-bonded complex **$P_{III}C_9/A_{II}F^*$** (30/70 mol), including the phase ranges of BPI and N*.

Fig. 6 shows the absorbance spectra obtained for the H-bonded complex **$P_{III}C_9/A_{II}F^*$** = 30/70 (mol) upon cooling (cooling rate = 0.5 °C/min). In fact, the absorbance peaks of LC phases (i.e., BPs and N*) in the H-bonded bent-core complex **$P_{III}C_9/A_{II}F^*$** = 30/70 (mol) were reflected away by the special pitches of BPI or chiral nematic phases. Importantly, no obvious absorbance peaks in H-bonded complex **$P_{III}C_9/A_{II}F^*$** = 30/70 (mol) were observed at higher temperature (115°C). However, a specific absorbance peak ca. 480 nm of H-bonded complex **$P_{III}C_9/A_{II}F^*$** = 30/70 (mol) appeared by decreasing temperatures to the range of 114-103°C, which could be assigned to the Bragg diffraction from the 110 plane of the cubic lattice in BPI.[22] A platelet texture of BPI was observed by POM over the same temperature range at 108°C (see Fig. 5i). Moreover, a broader absorbance peak around 570 nm (with another different pattern from that of BPI) in Fig. 6 corresponds to the selective diffraction of N*. The absorbance spectral changes were reversible during different heating and cooling cycles. Therefore, the BPI phase range of 114-103°C verified by the absorbance spectral changes of **$P_{III}C_9/A_{II}F^*$** was compatible with that observed by the characterization of POM textures.

Conclusions

We synthesized and prepared a series of H-boned bent-core LC diads (**T/D**=1) and complexes (**T/D**<1) consisting of pyridyl and benzoic acid derivatives as H-accepters **T** and H-donors **D**, respectively. The chiral nematic phase of H-boned bent-core LC diads (**T/D**=1) was induced by introducing the H-bonds on the covalent-bonded bent-core supramolecules, and the widest chiral nematic phase range of H-bonded bent-core diad **$P_{III}C_9/A_{II}F^*$** =1:1 was obtained by introducing the H-bond at the center of the bent-core supramolecule. Therefore, the longer alkyl chain of H-accepter and lateral fluoro group of H-donor would promote the chiral nematic phase ranges in H-bonded bent-core diads. The H-bonded bent-core complex **$P_{III}C_9/A_{II}F^*$** (3/7 mol/mol) showed the widest range of BPI (i.e., ΔT_{BP} = 12.0°C) upon cooling. As a result, the longer alkyl chain length of H-accepter and lateral fluoro group of H-donor could induce and stabilize the blue phase (BPI) range at special molar ratios of H-donor **$A_{II}F^*$** (55-80 mol%) in H-bonded bent-core complexes. Interestingly, the analogous covalent-bonded bent-core mixture **$P_{III}C_9A_{II}F^*/A_{II}F^*$** only induced the BPIII phase at molar ratios of **$A_{II}F^*$** = 75.0 to 82.4 mol%, rather than the BPI phase induced by the similar H-bonded bent-core complex **$P_{III}C_9/A_{II}F^*$** (3/7 mol/mol). Accordingly, we could summarize that the introduction of H-bonds in the bent-core center of the supramolecular complexes effectively induce and stabilize the BP phase. Moreover, not only the molar ratio of the chiral dopant affects the BPI range, but also the fluoro group of the proton donor directly affect the BPI formation of H-bonded bent-core complexes.

Acknowledgements

The financial supports of this project are provided by the Ministry of Science and Technology (MOST) in Taiwan through MOST103-2113-M-009-018-MY3 and MOST103-2221-E-009-215-MY3.

View Article Online
DOI: 10.1039/C5RA26827C
Journal Name

Notes and references

1 I. Fischer, N. Shah, A. Rosch, *Phys. Rev. B* 2008, **77**, 024415.
2 A. Yoshizawa, *RSC Adv*., 2013, **3**, 25475-25497.
3 W. Kossel, V. Loeck, H. Z. Voges, *A: Hadrons Nucl.,* 1935, **94**, 139.
4 R. J. Miller, H. F. Gleeson, J. E. Lydon, *Phys. Rev. Lett.,* 1996, **77**, 857-860.
5 R. M. Hornreich, S. Shtrikman, *Phys. Rev. A,* 1981, **24**, 635-638.
6 L. Longa, D. Monselesan, H. R. Trebin, *Liq. Cryst.,* 1989, **5**, 889-898.
7 P. Pieranski, R. B. Massin, P. E. Cladis, *Phys. Rev. A,* 1985, **31**, 3912-3923.
8 O. Henrich, K. Stratford, M. E. Cates, D. Marenduzzo, *Phys. Rev. Lett.,* 2011, **106**, No. 107801.
9 A. Yoshizawa, M. Kamiyama, T. Hirose, *Appl. Phys. Express,* 2011, **4**, No. 101701.
10 Y. F. Lan, C. Y. Tsai, J. K. Lu, N. Sugiura, *Opt. Express*, 2013, **21**, 5035-5040.
11 S. Meiboom, M. Sammon, *Phys. Rev. Lett*., 1980, **44**, 882-885.
12 M. Sato, A. Yoshizawa, *Adv. Mater.,* 2007, **19**, 4145-4148.
13 L. Rao, Z. Ge, S. T. Wu, *Opt. Express,* 2010, **18**, 3143-3148.
14 J. Yan, S. T. Wu, K. L. Cheng, J. W. Shiu, *Appl. Phys. Lett.,* 2013, **102**, No. 081102.
15 W. Cao, A. Munoz, P. P. Muhoray, B. Taheri, *Nat. Mater.,* 2002, **1**, 111-113.
16 K. Higashiguchi, K. Yasui, H. kikuchi, *J. Am. Chem. Soc.,* 2008, **130**, 6326-6327.
17 K. Kim, S. T. Hur, S. Kim, S. Y. Jo, B. R. Lee, M. H. Song, S. W. Choi, *J. Mater. Chem. C*, 2015, **3**, 5383-5388.
18 C. Y. Huang, J. J. Stott, R. G. Petschek, *Phys. Rev. Lett*., 1998, **80**, 5603-5606.
19 H. Y. Liu, C. T. Wang, C. Y. Hsu, T. H. Lin, J. H. Liu, *Appl. Phys. Lett.,* 2010, **96**, No. 121103.
20 F. Castles, F. V. Day, S. M. Morris, D. H. Ko, D. J. Gardiner, M. M. Qasim, S. Noheen, P. J. W. Hands, S. S. Choi, R. H. Friend, H. J. Coles, *Nat. Mater.,* 2012, **11**, 599-603.
21 P. P. Crooker in *Chirality in Liquid Crystals* (Eds.: H. S. Kitzerow, C. Bahr), Springer, **2001**, PP. 186-222.
22 H. Kikuchi, M. Yokota, Y. Hisakado, H. Yang, T. Kajiyama, *Nat. Mater.,* 2002, **1**, 64-68.
23 L. Wang, W. He, Q. Wang, M. Yu, X. Xiao, Y. Zheng, M. Ellahi, D. Zhao, H. Yang, L. Guo, *J. Mater. Chem. C*, 2013, **1**, 6526-6531.
24 J. Yan, S. T. Wu, *Opt. Mater. Express,* 2011, **1**, 1527-1535.
25 F. Peng, Y. Chen, J. Yuan, H. Chen, S. T. Wu, Y. Haseba, *J. Mater. Chem. C,* 2014, **2**, 3597-3601.
26 H. Yoshida, Y. Tanaka, K. Kawamoto, H. Kubo, T. Tsuda, A. Fujii, S. Kuwabata, H. Kikuchi, M. Ozaki, *Appl. Phys. Express,* 2009, **2**, No. 121501.
27 E. karatairi, B. Rozic, Z. Kutnjak, V. Tzitzios, G. Nounesis, G. Cordoyiannis, J. Thoen, C. Glorieux, S. Kralj, *Phys. Rev. E,* 2010, **81**, No. 041703.
28 L. A. Madsen, T. J. Dingemans, M. Nakata, E. T. Samulski, *Phys. Rev. Lett*., 2004, **92**, No. 145505.
29 H. Iwamochi, T. Hirose, Y. Kogawa, A. Yoshizawa, *Chem. Lett.,* 2010, **39**, 170-171.
30 M. Lee, S. T. Hur, H. Higuchi, K. Song, S. W. Choi, H. Kikuchi, *J. Mater. Chem.,* 2010, **20**, 5813-5816.
31 L. Wang, W. He, X. Xiao, Q. Yang, B. Yang, P. Li, H. Yang, *J. Mater. Chem.,* 2012, **22**, 2383-2386.
32 K. W. Park, M. J. Gim, S. Kim, S. T. Hur, S. W. Choi, ACS Appl. Mater. Interfaces, 2013, **5**, 8025-8029.
33 M. Grunert, R. A. Howie, A. Kaeding, C. T. Imrie, *J. Mater. Chem.,* 1997, **7**, 211-214.
34 J. Wang, Y. Shi, K. Yang, J. Wei, J. Guo, *RSC Adv*., 2015, **5**, 67357-67364.
35 W. L. He, G. H. Pan, Z. Yang, D. Y. Zhao, G. G. Niu, W. Huang, X. T. Yuan, J. B. Guo, H. Cao, H. Yang, *Adv. Mater*., 2009, **21**, 2050-2053.
36 E. Grelet, B. Pansu, M. H. Li, H. T. Nguyen, *Phys. Rev. Lett*., 2001, **86**, 3791-3794
37 H. J. Coles, M. N. Pivnenko, *Nature,* 2005, **436**, 997-1000.
38 J. Rokunohe, A. Yoshizawa, *J. Mater. Chem.,* 2005, **15**, 275-279.
39 A. Yoshizawa, Y. Kogawa, K. Kobayashi, Y. Takanishi, J. Yamamoto, *J. Mater. Chem.,* 2009, **19**, 5759-5764.
40 B. Y. Zhang, F. B. Meng, Y. H. Cong, *Opt. Express,* 2007, **15**, 10175-10181.
41 A. Hauser, M. Thieme, A. Saupe, G. Heppke, D. Kruerke, *J. Mater. Chem.,* 1997, **7**, 2223-2229.
42 O. Jin, D. Fu, J. Wei, H. Yang, J. Guo, *RSC Adv*., 2014, **4**, 28597-28600.
43 H. Y. Liu, C. T. Wang, C. Y. Hsu, T. H. Lin, J. H. Liu, *Appl. Phys. Lett.,* 2010, **96**, No. 121103.
44 A. Yoshizawa, Y. Kogawa, K. Kobayashi, Y. Takanishi, J. Yamamodo, *J. Mater. Chem.,* 2009, **19**, 5759-5764.
45 I. H. Chiang, C. J. Long, H. C. Lin, W. T. Chuang, J. J. Lee, H. C. Lin, *ACS Appl. Mater. Interfaces*, 2014, **6**, 228-235.
46 C. L. Wei, T. C. Chen, P. Raghunath, M. C. Lin, H. C. Lin, *RSC Adv*., 2015, **5**, 4615-4622.
47 P. L. Madhuri, S. K. Prasad, G. G. Nair, *RSC Adv.*, 2014, **4**, 3121-3130.
48 T. T. Nguyen, S. Albert, T. L. A. Nguyen, R. Deschenaux, *RSC Adv*., 2015, **5**, 27224-27228.
49 I. H. Chiang, W. T. Chuang, C. L. Lu, M. T. Lee, H. C. Lin, Chem. Mater., 2015, **27**, 4525-4537.
50 M. Caricato, A. K. Sharma, C. Coluccini, D. Pasini, *Nanoscale*, 2014, **6**, 7165-7174.
51 M. Caricato, A. Delforge, D. Bonifazi, D. Dondi, A. Mazzanti, D. Pasini, *Org. Biomol. Chem*., 2015, **13**, 3593-3601.
52 C. Coluccini, M. Caricatio, E. Cariati, S. Righetto, A. Forni, D. Pasini, *RSC Adv*., 2015, **5**, 21495-21503.
53 G. R. Luckhurst, *Angew. Chem. Int. Ed.* 2005, **44**, 2834-2836.
54 C. Tschierske, D. J. Photinos, *J. Mater. Chem.,* 2010, **20**, 4263-4294.
55 A. Yoshizawa, M. Sato, J. Rokunohe, *J. Mater. Chem.,* 2005, **15**, 3285-3290.
56 M. Sato, A. Yoshizawa, *Adv. Mater.,* 2007, **19**, 4145-4148.
57 M. Tanaka, A. Yoshizawa, *J. Mater. Chem. C*, 2013, **1**, 315-320.
58 R. Nomura, J. Tabei, T. Masuda, *J. Am. Chem. Soc.,* 2001, **123**, 8430-8431.
59 M. V. Sigalov, B. A. Shainyan, N. N. Chipanina, L. P. Oznobikhina, *J. Phys. Chem. A,* 2013, **117**, 11346-11356.
60 U. Kumar, T. Kato, J. M. J. Frechet, *J. Am. Chem. Soc.*, 1992, **114**, 6630-6639.

Journal Name

View Article Online
DOI: 10.1039/C5RA26827C ARTICLE

61 T. Kato, J. M. J. Frechet, P. G. Wilson, T. Saito, T. Uryu, A. Fujishima, C. Jin, F. Kaneuchi, *Chem. Mater.*, 1993, **5**, 1094-1100.

62 T. R. Shattock, K. K. Arora, P. Vishweshwar, M. J. Zaworotko, *Cryst. Growth Des.,* 2008, **8**, 4533-4545.

63 Y. Zhang, Y. Guan, S. Yang, J. Xu, C. C. Han, *Adv. Mater.,* 2003, **15**, 832-835.

64 Y. Li, Y. Cong, H. Chu, B. Zhang, *J. Mater. Chem. C*, 2014, **2**, 1783-1790.

65 W. H. Binder, S. Bernstorff, C. Kluger, L. Petraru, M. J. Kunz, *Adv. Mater.,* 2005, **17**, 2824-2828.

66 J. Huo, Y. Shi, X. Han, O. Jin, J. Wei, H. Yang, *J. Mater. Chem. C*, 2013, **1**, 947-957.

67 W. L. He, G. H. Pan, Z. Yang, D. Y. Zhao, G. G. Niu, W. Huang, X. T. Yuan, J. B. Guo, H. Cao, H. Yang, *Adv. Mater*., 2009, **21**, 2050-2053.

68 L. Y. Wang, I. H. Chiang, P. J. Yang, W. S. Li, I. T. Chao, H. C. Lin, *J. Phys. Chem. B,* 2009, **113**, 14648-14660.

69 L. Y. Wang, H. Y. Tsai, H. C. Lin, *Macromolecules,* 2010, **43**, 1277.

70 C. Osuji, C. Y. Chao, I. Bita, C. K. Ober and E. L. Thomas, *Adv. Funct. Mater.*, 2002, **12**, 753–758.

71 B. Basu, *RSC Adv*., 2014, **4**, 13854-13881.

72 L. Y. Wang, S. Y. Tsa and H. C. Lin, *Macromolecules*, 2010, **43**, 1277–1288.

73 P. J. Yang, L. Y. Wang, C. Y. Tang and H. C. Lin, *J. Polym. Sci., Part A: Polym. Chem.*, 2010, **48**, 764–774.

ARTICLE View Article Online DOI: 10.1039/C5RA26827C Journal Name

For Table of Contents/Abstract Graphic Use Only

Hydrogen-bonded bent-core blue phase liquid crystal complexes containing various molar ratios of proton acceptors and donors

Chun-Chieh Han, Yu-Chaing Chou and Hong-Cheu Lin*

Department of Materials Science and Engineering, National Chiao Tung University, Hsinchu, Taiwan

Table of Contents (TOC)/ABSTRACT Graphic

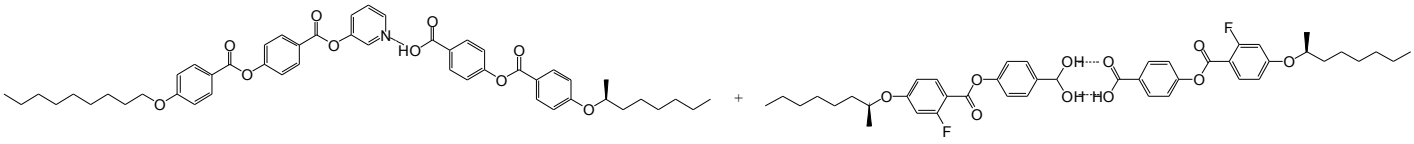

$P_{III}C_9/A_{II}F^*$ = 3/7 mol/mol

Iso 114.5 [0.25] BPI 102.5 N* 67.3 [1.60] K (BPI = 12°C)

In BPLC complexes, the molar ratios, alkyl chain lengths, the lateral fluoro-substitution and the chiral center of H-bonded bent-core supramolecules would affect their temperature ranges of BPs. H-bonded bent-core complex **$P_{III}C_9/A_{II}F^*$** (3/7 mol/mol) displayed the widest BPI ranges of ΔT_{BPI} = 12.0°C at the correspondent H-accepter **T** = **$P_{III}C_9$** (with the longest alkyl chain length **C_9**) and H-donor **D** = **$A_{II}F^*$** (with a lateral fluoro-substitution and a chiral center).

